

# Camera-Agnostic Pruning of 3D Gaussian Splats via Descriptor-Based Beta Evidence

Peter Fasogbon<sup>1</sup>  
peter.fasogbon@nokia.com

Ugurcan Budak<sup>1</sup>  
ugurcan.budak.ext@nokia.com

Patrice Rondao Alface<sup>2</sup>  
patrice.rondao\_alface@nokia.com

Hamed R. Tavakoli<sup>1</sup>  
hamed.rezazadegan\_tavakoli@nokia.com

<sup>1</sup> Nokia Technologies,  
Espoo, Finland

<sup>2</sup> Nokia Technologies,  
Antwerp, Belgium

## Abstract

The pruning of 3D Gaussian splats is essential for reducing their complexity to enable efficient storage, transmission, and downstream processing. However, most of the existing pruning strategies depend on camera parameters, rendered images, or view-dependent measures. This dependency becomes a hindrance in emerging camera-agnostic exchange settings, where splats are shared directly as point-based representations (e.g., .ply). In this paper, we propose a *camera-agnostic, one-shot, post-training* pruning method for 3D Gaussian splats that relies solely on attribute-derived neighbourhood descriptors. As our primary contribution, we introduce a hybrid descriptor framework that captures structural and appearance consistency directly from the splat representation. Building on these descriptors, we formulate pruning as a statistical evidence estimation problem and introduce a *Beta evidence* model that quantifies per-splat reliability through a probabilistic confidence score.

Experiments conducted on standardized test sequences defined by the ISO/IEC MPEG Common Test Conditions (CTC) demonstrate that our approach achieves substantial pruning while preserving reconstruction quality, establishing a practical and generalizable alternative to existing camera-dependent pruning strategies.

## Introduction

3D Gaussian Splatting (3DGS) has recently emerged as a powerful representation for real-time novel view synthesis, achieving high visual fidelity by modelling scenes as collections of anisotropic Gaussian primitives [1]. By enabling fast rasterization and high-quality rendering, 3DGS has quickly become a competitive alternative to neural radiance fields (NeRFs) [2] for interactive applications. However, realistic scenes often require hundreds of thousands to millions of splats, leading to substantial storage costs, increased memory footprint, and higher computational overhead. These characteristics limit the practical deployment of

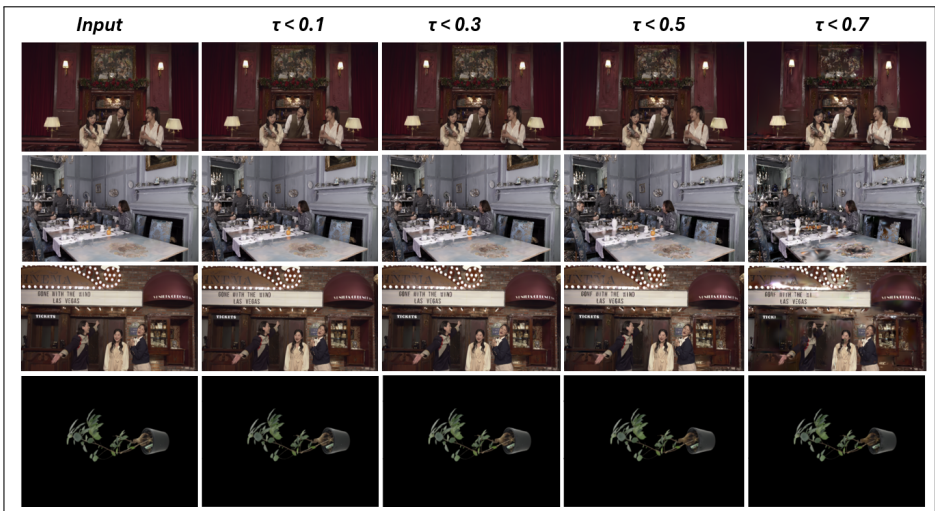


Figure 1: Overview of the proposed Gaussian splat pruning method on an example scene from the ISO/IEC MPEG CTC dataset [8], rendered from a fixed camera viewpoint. The image columns show the non-pruned baseline and increasing pruning thresholds  $\tau = 0.1, 0.3, 0.50$ , and  $0.7$ , which remove about 10%, 30%, 50%, and 70% of splats, respectively.

3DGS models on resource-constrained platforms such as mobile devices, embedded systems, and bandwidth-limited streaming scenarios.

To address this challenge, pruning and compression of Gaussian splats have become active research topics. A prominent post-training prune-recover methodology in LightGaussian [2] estimates global splat significance, performs spherical harmonics distillation, and applies vector quantization as part of an integrated compression pipeline. This approach achieves substantial model size reduction while largely preserving rendering quality. Similarly, Confident Splatting [19] introduces confidence-aware pruning by learning per-splat Beta distributions during training, using view-dependent reconstruction signals to guide opacity modulation and pruning decisions. Despite their effectiveness, these approaches fundamentally rely on training-time supervision and camera-dependent information. Such assumptions do not hold in emerging MPEG standardization activities, notably within the Immersive 3D Gaussian Splatting (I-3DGS) paradigm [4], where Gaussian splats are exchanged directly as geometry-based point representations (e.g., `.ply` files) without access to training images, camera intrinsics, or extrinsics. In these interchange scenarios, pruning must operate purely post-training and remain fully camera-agnostic.

Unlike Confident Splatting, where Beta distribution parameters are learned jointly with splat parameters during training, our approach estimates Beta evidence entirely *post-training* from descriptor-derived statistics. In this work, we propose a *camera-agnostic, one-shot, post-training* pruning framework for 3D Gaussian splats. We formulate pruning as a statistical evidence estimation problem and derive per-splat confidence from the Hybrid Splat Feature Histogram (HSFH) descriptors computed directly from the learned Gaussian representation. This design ensures full compatibility with MPEG I-3DGS interchange pipelines

while preserving important structures under aggressive redundancy removal. Figure 1 illustrates the qualitative effect of the proposed method on some representative scene from the ISO/IEC MPEG CTC [8]. As the pruning threshold increases, progressively more low-confidence splats are removed. The visual quality remains largely preserved across moderate thresholds  $\tau$ , with noticeable degradation appearing only under aggressive pruning threshold.

## 2 Background and Related Work

3DGS [10] models a scene as a set of anisotropic Gaussian primitives parameterized by 3D position, covariance, opacity, and view-dependent appearance (e.g. spherical harmonics). The rendering is performed via differentiable rasterization and alpha compositing, enabling real-time performance while maintaining high visual fidelity. Unlike classical point clouds, each Gaussian splat carries anisotropic spatial support and learned radiance parameters. Therefore, splat importance is not purely geometric and thus depends jointly on its covariance structure, opacity, and appearance. This coupling between geometry and appearance complicates redundancy estimation compared to traditional mesh or point-based simplification. Furthermore, 3DGS splats are optimized for rendering rather than explicit geometric reconstruction. As a result, heuristics designed for point decimation or mesh simplification do not directly transfer to Gaussian-based representations.

### 2.1 Pruning in 3DGS

Existing pruning strategies for 3DGS can be categorised by the technique used to estimate splat importance.

**Training-Stage Pruning.** The original 3DGS framework [10] prunes Gaussians during optimization based on opacity thresholds, excessive scale growth, or negligible gradient contribution. Since these criteria depend on rendering loss and view visibility, they are inherently tied to training trajectories. Subsequent methods, such as BOGausS [16], track training-stage behaviours to improve optimization efficiency while implicitly removing unimportant splats. Mini-Splatting [9] and EAGLES [5] prioritize Gaussians using visibility and contribution statistics accumulated from training views. RAP [25] trains a lightweight MLP during optimization to infer per-Gaussian confidence scores, while using rendering supervision to guide importance estimation. These approaches remain tightly coupled to gradient-based optimization and camera-dependent rendering signals.

**Gradient-Based and Learned Pruning.** More recent methods introduce differentiable or learned importance estimation. LP-3DGS [26] learns a binary pruning mask via a Gumbel-Sigmoid relaxation, requiring iterative joint optimization. PUP-3DGS [6] employs second-order sensitivity analysis based on Hessian approximations to score Gaussians. Opacity-assisted pruning [18] and semantic-guided approaches such as Clean-GS [15] similarly depend on training-time gradients, visibility statistics, or segmentation masks. Although these strategies achieve strong compression-performance trade-offs, they require access to training views, camera parameters, or optimization signals.

**Post-Training Compression Pipelines.** Post-training compression has also been explored in the literature. LightGaussian [2] combines global significance-based pruning with spher-

ical harmonics distillation and vector quantization. While effective, its significance estimation and recovery stages rely on rendering evaluation driven by camera parameters. Confident Splatting [19] introduces a probabilistic confidence model by jointly learning per-splat Beta distributions during training. This provides principled uncertainty-aware pruning, but requires modifying the training procedure and leveraging view-dependent reconstruction signals.

**Structural and Feature-Space Pruning.** Some approaches target latent or structural components instead of splats directly. Hash Grid Feature Pruning [13] removes unused hash-grid feature entries by analyzing geometric support from Gaussian centers. Adversarial Pruning Networks (APNet) [21] apply adversarial learning to prune Gaussians in a data-driven manner. These methods reduce redundancy in auxiliary representations but either rely on supervised retraining or do not operate directly on the Gaussian primitives themselves.

**NeRF and Visibility-Based Pruning.** Related work in NeRF compression prunes network weights, hash grids, or spatial regions based on ray-based saliency. Examples include coreset-based neuron pruning [0], HollowNeRF [23], and visibility-driven geometry pruning [8]. While conceptually related, these methods operate on neural field representations and depend on ray sampling or view statistics.

## 2.2 Intrinsic Cues from Local Structure

When importance must be inferred from the Gaussian representation itself, redundancy estimation must rely on intrinsic structural cues. In classical 3D vision, local reliability is commonly derived from neighborhood descriptors computed over point clouds or surface patches. Hand-crafted descriptors such as Spin Images [9], SHOT [22], and Fast Point Feature Histograms (FPFH) [20] encode geometric consistency within local neighborhoods and have been widely used for registration and robustness analysis. In addition, learning-based point descriptors, including PointNet-family encoders [17] and contrastive local embeddings [24], further demonstrate that neighbourhood structure provides informative signals even in the absence of camera information.

However, Gaussian splats differ fundamentally from raw points: they incorporate anisotropic covariance, opacity, and radiance parameters optimized for differentiable rendering. Descriptor-driven reliability estimation tailored specifically to Gaussian primitives remains largely unexplored. This motivates this work to propose splat-aware neighbourhood descriptors that jointly capture geometric and appearance consistency.

## 2.3 Positioning of This Work

Our work addresses the post-training regime in which only a finalized set of Gaussian splats (e.g., a .ply asset) is available, without access to cameras, rendered images, or training-time gradients. In contrast to camera-dependent prune-and-recover pipelines [0], training-coupled confidence learning [19], and joint optimization frameworks [12], we propose a strictly camera-agnostic pruning strategy that operates entirely on the learned Gaussian representation.

Conceptually, our method follows a two-stage formulation. First, importance is inferred from intrinsic splat-aware neighborhood descriptors computed directly from Gaussian pa-

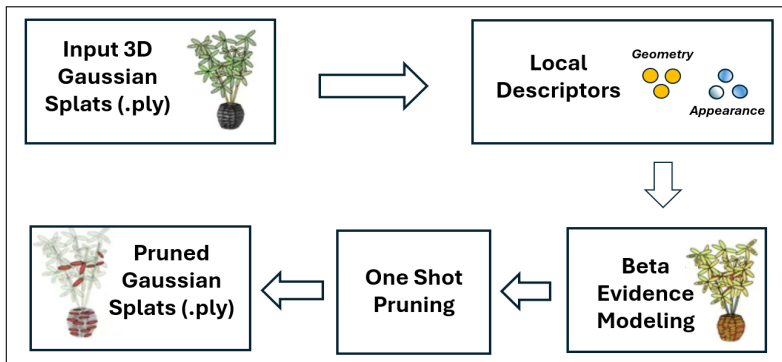


Figure 2: Method overview of the proposed camera-agnostic Gaussian splat pruning framework. Given trained 3D Gaussian splats, local descriptor statistics are computed and transformed into Beta-distributed evidence to model confidence and uncertainty. A one-shot confidence-aware ranking then removes redundant splats, balancing expected pruning likelihood and uncertainty to produce the final pruned representation.

rameters, without rendering supervision. Second, these descriptor signals are interpreted through a probabilistic Beta evidence model to estimate confidence and uncertainty for each splat. This separation between intrinsic structural measurement and statistical evidence interpretation enables one-shot pruning without retraining, recovery optimization, or camera visibility signals.

### 3 Proposed Method

The overall pipeline of the proposed method is illustrated in Figure 2. Given a trained set of Gaussians, our method proceeds in three stages: (1) computation of splat-aware neighborhood descriptors that capture intrinsic geometric and appearance consistency; (2) probabilistic confidence estimation via a Beta evidence model derived from descriptor statistics; and (3) one-shot ranking and pruning using an uncertainty-aware confidence criterion.

#### 3.1 Local Descriptor Extraction using HSFH

For a trained 3DGS representation, individual splat parameters are often insufficient for robust reliability inference. Instead, reliability is assessed from local neighborhood consistency. For each splat  $g_i$ , we compute a Gaussian splat descriptor  $\mathcal{D}_i$  over its spatial neighborhood  $\mathcal{N}(i)$ , capturing geometric and appearance relationships among nearby splats. Each splat is characterized by its position, covariance, opacity, and spherical harmonics appearance coefficients.

To effectively capture splat reliability, we introduce the HSFH, a descriptor tailored to Gaussian splatting representations. HSFH extends the PPFH descriptor [24] by incorporating appearance cues derived from spherical harmonics.

**Geometric component.** The geometric component encodes local shape using histograms of Darboux frame angles  $(\alpha, \sigma, \theta)$ , as in PPFH. For each splat, the angles between surface

normals and relative neighbor directions are quantized into three 11-bin histograms, which are concatenated to form a 33-dimensional geometric descriptor. This representation captures local curvature, anisotropy, and relative orientation, and is robust to noise and irregular point distributions.

**Appearance component from spherical harmonics.** Appearance cues are derived from the spherical harmonics coefficients associated with each splat using two complementary encodings:

1. *Power spectrum  $P_\ell$ .* Band-wise energy is computed for each spherical harmonics degree  $\ell$ , which provides a compact summary of radiance variation across angular frequencies.

$$P_\ell = \sum_{m=-\ell}^{\ell} \|c_{\ell m}\|^2,$$

2. *Histogram representation.* Spherical harmonics coefficients (or reconstructed color responses) are discretized into fixed bins to capture the distribution of local appearance variation within the neighborhood.

Both encodings are normalized and concatenated with the geometric descriptor to form the final camera-agnostic HSFH representation.

**Optional view-aware features.** When camera information is available, HSFH can be augmented with a low-dimensional component describing splat-view alignment. For each splat and camera, we compute: (i) the Euclidean distance between the splat center and the camera center, (ii) the cosine of the angle between the splat normal and the viewing direction, and (iii) the alignment between the splat orientation and the camera forward axis. These quantities are concatenated into a compact 10-dimensional vector that captures relative distance, angular alignment, and orientation.

In strictly camera-agnostic settings, this view-aware component is omitted, and HSFH reduces to geometry and appearance features only. When available, view-aware cues provide additional retention evidence for grazing-angle splats and fine structures.

## 3.2 Beta Evidence Modeling

We model the splat pruning as a probabilistic decision under uncertainty. For each splat  $g_i$ , we define a Bernoulli random variable indicating whether the splat should be pruned, and model uncertainty using a Beta distribution,

$$p_i \sim \text{Beta}(A_i, B_i), \quad (1)$$

where  $A_i$  represents evidence supporting *retention* of splat  $i$  and  $B_i$  represents evidence supporting *safe pruning*. Beta distributions provide a principled representation of uncertainty for binary decisions and are widely used in uncertainty-aware learning and decision-making [14].

The posterior mean

$$\mu_i = \frac{B_i}{A_i + B_i} \quad (2)$$

corresponds to the expected pruning probability, while the variance

$$\sigma_i^2 = \frac{A_i B_i}{(A_i + B_i)^2 (A_i + B_i + 1)} \quad (3)$$

captures the associated uncertainty.

**Descriptor-derived statistics and evidence mapping.** For each splat  $g_i$ , we compute a set of normalized scalar statistics  $s_i, \ell_i, o_i, u_i \in [0, 1]$  derived from descriptor aggregation over its spatial neighborhood  $\mathcal{N}(i)$ . These statistics summarize local geometric and appearance consistency:

- $\ell_i$  measures *low geometric contrast*, computed as the inverse normalized standard deviation of the geometric descriptor block, such that homogeneous neighbourhoods yield high values.
- $s_i$  measures *low-frequency appearance consistency*, computed as the inverse normalized variance of appearance-related descriptor components.
- $o_i$  denotes the normalized splat opacity.
- $u_i$  denotes a *geometry uniqueness* score, computed from the variability of descriptor components across dimensions, with higher values indicating structurally distinctive neighbourhoods.

These statistics are accumulated as soft evidence in the Beta model using distance-weighted aggregation in equation (4), where  $w$  denotes an aggregation weight.

$$\begin{aligned} B_i &\leftarrow B_i + w(0.50 s_i + 0.35 \ell_i + 0.20(1 - o_i)) + 0.20(1 - u_i), \\ A_i &\leftarrow A_i + w(0.55 o_i) + 0.50 u_i, \end{aligned} \quad (4)$$

The weighting coefficients are selected empirically and reflect the relative importance of geometric homogeneity, appearance consistency, opacity, and structural distinctiveness for pruning reliability. Homogeneous neighbourhoods with low geometric and appearance variation increase pruning evidence, while opaque and structurally distinctive splats increase retention evidence. The formulation is flexible and can be tuned to emphasize geometry, appearance, or opacity depending on the target application.

**Optional camera-aware extensions.** When camera information is available, an additional grazing or edge-likeness proxy  $e_i$  can be computed from normal-view alignment and opacity statistics. This term provides supplementary retention evidence for splats located near silhouettes, contours, or grazing-angle configurations.

In strictly camera-agnostic settings, this term is omitted. Importantly, effective pruning is achieved without any view-dependent information, and optional camera-aware cues serve only as auxiliary refinements when available.

### 3.3 One-Shot Pruning

A pruning decision can be derived from the lower confidence bound (LCB) of the Beta posterior in equation (5) where  $q$  is a user-defined quantile.

$$\text{LCB}_i = \text{BetaInvCDF}(q, A_i, B_i), \quad (5)$$

In practice, we approximate the LCB using a Gaussian moment form in equation (6), where  $\mu_i$  and  $\sigma_i$  denote the posterior mean and standard deviation, and  $z$  controls the confidence level.

$$\text{LCB}_i \approx \mu_i - z \sigma_i. \quad (6)$$

However, the formulation in equation (6) is pessimistic, as it penalizes uncertainty by lowering the score of high-variance components. When applied to pruning, such a rule removes uncertain coefficients early and therefore results in aggressive pruning. To avoid over-pruning fine structures and semi-transparent regions, we employ an *optimistic confidence* inspired by the upper confidence bound (UCB) principle and shown in equation (7), where  $\gamma$  controls the confidence level and is defined by the user. This *score* softly rewards uncertainty and empirically stabilizes PSNR and SSIM under a high pruning ratio.

$$\text{score}_i = \mu_i + \gamma \sigma_i, \quad (7)$$

Finally, pruning is applied once by thresholding the confidence score using a condition in equation (8), where  $\tau$  is the threshold defined by the user and initialized in the next section.

$$g_i \text{ is pruned if } \text{score}_i < \tau. \quad (8)$$

## 4 Experiments

In this section, we evaluate the proposed method on multiple MPEG CTC test sequences. All experiments are conducted strictly *post-training*, using the exported Gaussian splat representations (.ply). Our evaluation isolates the impact of two core components of the proposed framework: (i) descriptor-based neighbourhood modelling and (ii) probabilistic Beta evidence accumulation. We perform a systematic comparison against two camera-dependent state-of-the-art pruning baselines, as well as an ablation study analyzing the contribution of each component.

For controlled comparison, we construct pruning-only variants of two camera-dependent compression frameworks by isolating the pruning stages of LightGaussian [14] and Confident Splatting [19], excluding additional compression components such as quantization or recovery optimization. These reduced variants are denoted *LightGSPrune* and *ConfSplatPrune*. Both baselines rely on image-based supervision and therefore operate with access to optimization viewpoints, which may favour evaluation on the same views due to direct alignment with observed image projections. To avoid this potential bias, all methods are evaluated exclusively on held-out camera views that are not used during pruning or optimization, following the MPEG CTC evaluation protocol. The reconstruction quality is measured using PSNR, SSIM, and LPIPS. The non-pruned 3DGS model serves as the 100% quality reference, and all reported metrics quantify the deviation from this baseline after pruning.

## 4.1 Implementation Details

Since the pruning decisions are derived from descriptor-level statistics rather than raw Gaussian parameters, local descriptors are computed using the proposed HSFH (Section 3.1), and probabilistic confidence is estimated from aggregated descriptor statistics using the Beta evidence model (Section 3.2). To improve efficiency on large-scale scenes, descriptor computation is accelerated via voxelized downsampling. Unless otherwise specified, the voxel size is set to 1–2% of the scene bounding box diagonal, providing a practical trade-off between computational cost and preservation of local structure. Descriptors and statistics are computed at the voxel level and interpolated to individual splats using distance-based weighting, so that final pruning decisions are always applied at full splat resolution.

The pruning is controlled by the confidence threshold  $\tau$  and uncertainty weight  $\gamma$  (Section 3.3).  $\tau$  is selected via percentile thresholding to achieve a target pruning ratio (e.g.,  $\tau \approx 0.30$  and  $\tau \approx 0.10$  yield approximately 30% and 10% pruning). The uncertainty weight is fixed to  $\gamma = 0.25$  in all experiments.

## 4.2 Quantitative Comparison

We evaluate the proposed camera-agnostic pruning method against two state-of-the-art pruning baselines, *LightGSPrune* and *ConfSplatPrune*, derived from the *LightGaussian* [2] and *Confident Splatting* [19] frameworks, respectively. All methods are evaluated with our method *BetaDescPrune* relative to the non-pruned 3DGS model, which serves as the 100% quality reference.

The experimental results reported in Table 1 reflect performance under this shared evaluation setting. At low and medium pruning levels, camera-aware methods generally achieve the highest reconstruction fidelity, reflecting their use of view-dependent supervision. Nevertheless, the proposed camera-agnostic approach remains competitive despite operating without access to image projections. At the highest pruning ratio, the proposed method achieves slightly better performance on the *breakfast (tracked)* and *cinema (tracked)* sequences, which exhibit complex spatial layouts and diverse viewpoint coverage. These large-scale scenes contain substantial spatial redundancy, making high-ratio pruning more meaningful and allowing the descriptor-driven confidence modelling to effectively remove structurally redundant splats while preserving geometry.

In contrast, performance remains near-saturated on the object-centric *plant* sequence across all methods. Such scenes typically contain a relatively small number of splats and exhibit structured, compact geometry with limited spatial variability. Consequently, aggressive pruning yields diminishing returns, and lower pruning ratios are generally more appropriate for this type of dataset. This observation indicates that the proposed method is particularly well-suited for large-scale, spatially diverse environments where redundancy is more pronounced, while object-centric scenes with limited splat counts naturally benefit from conservative pruning. Overall, these results demonstrate that descriptor-driven neighbourhood modelling, coupled with uncertainty-aware confidence estimation, enables effective structure-preserving pruning without reliance on view-dependent supervision, particularly in large and geometrically complex scenes.

Dataset	Metric	Camera-Aware Methods						Our Method		
		<i>ConfSplatPrune</i>			<i>LightGSPrune</i>			<i>BetaDescPrune</i>		
		Low	Mid	High	Low	Mid	High	Low	Mid	High
bartender (tracked)	PSNR ( $\uparrow$ )	89.83	86.03	85.07	89.81	86.13	85.05	88.52	86.01	84.10
	SSIM ( $\uparrow$ )	0.991	0.990	0.985	0.992	0.990	0.983	0.990	0.982	0.973
	LPIPS ( $\downarrow$ )	0.015	0.028	0.031	0.015	0.029	0.030	0.019	0.034	0.049
breakfast (tracked)	PSNR ( $\uparrow$ )	89.02	84.12	80.07	88.03	84.10	79.74	86.12	83.24	<b>81.12</b>
	SSIM ( $\uparrow$ )	0.992	0.981	0.946	0.991	0.981	0.945	0.988	0.975	<b>0.962</b>
	LPIPS ( $\downarrow$ )	0.021	0.026	0.057	0.020	0.027	0.060	0.015	0.029	<b>0.043</b>
cinema (tracked)	PSNR ( $\uparrow$ )	86.95	86.23	78.09	87.05	86.49	78.12	84.07	81.34	<b>79.92</b>
	SSIM ( $\uparrow$ )	0.989	0.987	0.940	0.990	0.989	0.942	0.982	0.969	<b>0.954</b>
	LPIPS ( $\downarrow$ )	0.011	0.016	0.066	0.010	0.014	0.066	0.022	0.040	<b>0.057</b>
plant	PSNR ( $\uparrow$ )	97.05	97.05	97.01	97.06	97.05	96.99	96.72	93.26	90.58
	SSIM ( $\uparrow$ )	0.999	0.999	0.998	0.999	0.999	0.998	0.999	0.998	0.997
	LPIPS ( $\downarrow$ )	0.001	0.001	0.001	0.001	0.001	0.001	0.001	0.002	0.003

Table 1: Comparison with prior pruning methods at low (10%), medium (20%), and high (30%) pruning ratios. Higher PSNR and SSIM indicate better reconstruction quality, while lower LPIPS is better. All methods are evaluated on held-out camera views not used during pruning.

Dataset	Metric	No Descriptors		With Descriptors	
		No Beta	Beta	No Beta	Beta
bartender (tracked)	PSNR ( $\uparrow$ )	79.91	84.23	78.88	<b>86.07</b>
	SSIM ( $\uparrow$ )	0.955	0.979	0.948	<b>0.982</b>
	LPIPS ( $\downarrow$ )	0.055	0.035	0.074	<b>0.034</b>
breakfast (tracked)	PSNR ( $\uparrow$ )	74.98	83.90	72.94	<b>84.47</b>
	SSIM ( $\uparrow$ )	0.933	0.978	0.903	<b>0.979</b>
	LPIPS ( $\downarrow$ )	0.072	0.027	0.097	<b>0.025</b>
cinema (tracked)	PSNR ( $\uparrow$ )	76.76	82.15	74.45	<b>82.16</b>
	SSIM ( $\uparrow$ )	0.937	0.970	0.925	<b>0.972</b>
	LPIPS ( $\downarrow$ )	0.075	0.037	0.091	<b>0.036</b>
plant	PSNR ( $\uparrow$ )	89.73	93.05	89.73	<b>93.05</b>
	SSIM ( $\uparrow$ )	0.995	0.998	0.995	<b>0.998</b>
	LPIPS ( $\downarrow$ )	0.005	0.002	0.005	<b>0.002</b>

Table 2: Ablation study evaluating the impact of descriptor-based modeling and Beta uncertainty estimation on pruning performance. Higher PSNR and SSIM indicate better reconstruction quality; lower LPIPS is better.

### 4.3 Ablation Study

To evaluate the contribution of individual components, we compare four pruning configurations: (i) pruning without descriptors or Beta modelling, (ii) pruning without descriptors but with Beta modelling, (iii) pruning with descriptors but without Beta modelling, and (iv) the full method combining descriptors with Beta evidence accumulation. Across all evaluated datasets, descriptor-based neighbourhood modelling improves pruning stability by incorporating local structural context beyond individual splat parameters. Incorporating Beta evidence modelling further enhances robustness through uncertainty-aware confidence estimation, reducing over-pruning in ambiguous regions. The full method consistently achieves the best reconstruction quality, demonstrating that structural descriptors and probabilistic uncertainty modeling provide complementary benefits for camera-agnostic pruning.

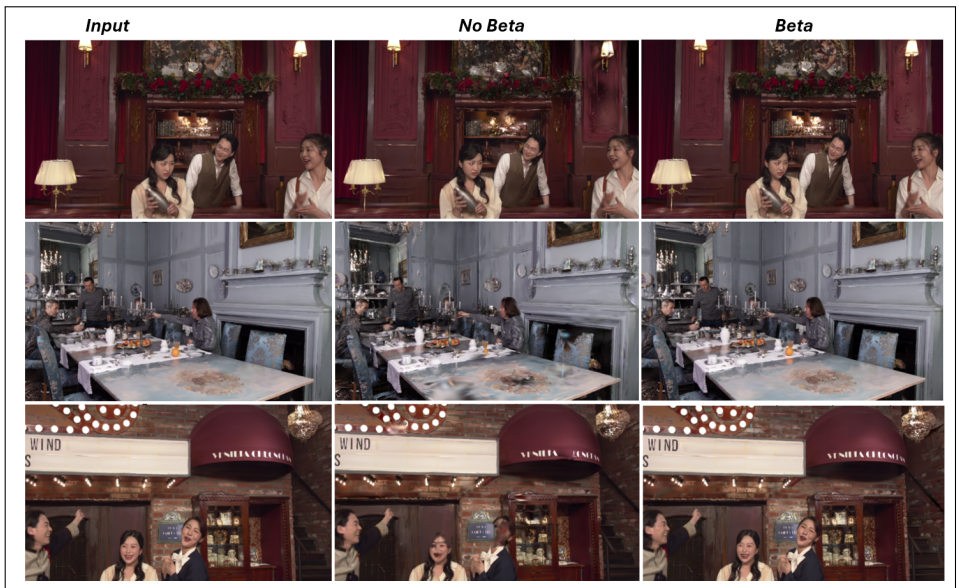


Figure 3: Qualitative comparison of camera-agnostic pruning on three MPEG CTC scenes (*bartender (tracked)*, *breakfast (tracked)*, *cinema (tracked)*) at approximately 20% pruning. The columns show (left to right) the input rendering, descriptor-only pruning without Beta modelling (No Beta), and uncertainty-aware pruning with Beta evidence (Beta). Incorporating Beta evidence improves preservation of fine structures and reduces visible pruning artefacts.

#### 4.4 Visual Analysis

Figure 3 shows qualitative results on three MPEG CTC scenes: *bartender (tracked)*, *breakfast (tracked)*, and *cinema (tracked)*, at approximately 20% pruning. The columns show the input rendering, descriptor-only pruning without Beta modelling (No Beta), and uncertainty-aware pruning with Beta evidence (Beta). The descriptor-only pruning removes redundant splats but introduces visible artefacts, particularly in thin structures, semi-transparent regions, and high-frequency geometric details. These appear as structural discontinuities and loss of fine geometry. Incorporating Beta evidence produces cleaner reconstructions with improved preservation of fine structures and more stable semi-transparent regions. Thus, accounting for uncertainty in the pruning decision leads to more consistent structure retention despite operating without camera information.

These qualitative results align with the quantitative findings, showing that uncertainty-aware pruning improves visual fidelity and reduces pruning artefacts, particularly in geometrically complex regions.

#### 4.5 Evaluation on Full CTC Dataset

To further validate the generalization capability of the proposed method, we extend the evaluation to all mandatory MPEG CTC sequences. The dataset consists of 19 sequences in total, including 7 forward-facing dynamic scenes and 12 object-centric scenes. We report

averaged performance separately for forward-facing and object-centric categories to account for their distinct structural characteristics. Metrics are averaged across all sequences within each category at fixed pruning ratios of 10%, 20%, and 30%.

For forward-facing scenes, the proposed method achieves an average PSNR of 90.15 dB, 87.21 dB, and 85.13 dB at 10%, 20%, and 30% pruning, respectively. The corresponding SSIM values are 0.989, 0.982, and 0.969, while LPIPS values are 0.019, 0.034, and 0.050. For object-centric scenes, the method achieves an average PSNR of 97.95 dB, 94.52 dB, and 90.30 dB at 10%, 20%, and 30% pruning, respectively, with SSIM values of 0.999, 0.998, and 0.997, and LPIPS values of 0.001, 0.002, and 0.003. The method shows particularly stable behavior on forward-facing dynamic scenes, where spatial redundancy is higher.

## 5 Conclusion and Future Work

We presented a camera-agnostic, one-shot, post-training pruning framework for 3DGS based on descriptor-driven Beta evidence. By operating directly on exported Gaussian representations and eliminating reliance on camera parameters, rendered images, or training-time supervision, the proposed method enables robust and reproducible pruning in interchange-oriented settings such as the MPEG I-3DGS paradigm. The experiments on standard MPEG test sequences show that substantial redundancy can be removed while preserving reconstruction quality, even without view-dependent information. These findings demonstrate that reliable splat confidence can be inferred from intrinsic neighborhood structure alone and that effective post-training pruning does not require camera supervision. The one-shot and deterministic formulation further ensures low computational overhead, making the method well-suited for large-scale and standardized processing pipelines.

An important direction for future work is to investigate how descriptor-driven confidence estimation interacts with downstream compression and transmission stages. In particular, integrating confidence-aware pruning with geometry and attribute coding, adaptive quantization, and rate-distortion optimization offers a promising path toward improved end-to-end efficiency in immersive Gaussian splatting systems.

## References

- [1] Tianqi Ding, Dawei Xiang, Pablo Rivas, and Liang Dong. Coreset-based neuron pruning halves nerf model size and speeds training by 35%. *arXiv preprint arXiv:2504.00950*, 2025. doi: 10.48550/arXiv.2504.00950.
- [2] Zhiwen Fan, Kevin Wang, Kairun Wen, Zehao Zhu, Dejia Xu, and Zhangyang Wang. Lightgaussian: unbounded 3d gaussian compression with 15x reduction and 200+ fps. In *Proceedings of the 38th International Conference on Neural Information Processing Systems*, NIPS '24, 2024. ISBN 9798331314385.
- [3] Guangchi Fang and Bing Wang. Mini-splatting: Representing scenes with a constrained number of gaussians. In *Computer Vision – ECCV 2024*, volume 15135 of *Lecture Notes in Computer Science*, pages 165–181. Springer, 2024. doi: 10.1007/978-3-031-72980-5\_10.

- [4] Davi R. Freitas, Ioan Tabus, and Christine Guillemot. Visibility-based geometry pruning of neural plenoptic scene representations. *IEEE Transactions on Multimedia*, 28: 1–16, 2026. doi: 10.1109/TMM.2025.3618548.
- [5] Sharath Girish, Kamal Gupta, and Abhinav Shrivastava. Eagles: Efficient accelerated 3d gaussians with lightweight encodings. In *Computer Vision – ECCV 2024*, volume 15121 of *Lecture Notes in Computer Science*, pages 54–71. Springer, 2024. doi: 10.1007/978-3-031-73036-8\_4.
- [6] Alex Hanson, Allen Tu, Vasu Singla, Mayuka Jayawardhana, Matthias Zwicker, and Tom Goldstein. Pup 3d-gs: Principled uncertainty pruning for 3d gaussian splatting. In *CVPR*, 2025.
- [7] ISO/IEC JTC 1/SC 29/WG 2 (MPEG). Gaussian splat coding requirements. <https://www.mpeg.org>, 2025. Document N0487, 152nd MPEG Meeting, Geneva, October 2025.
- [8] ISO/IEC JTC 1/SC29/WG4 (MPEG). Common test conditions (ctc) for gaussian splat coding. <https://www.mpeg.org>, 2025. Document N0752, 152nd MPEG Meeting, Geneva, October 2025.
- [9] Andrew E. Johnson and Martial Hebert. Using spin images for efficient object recognition in cluttered 3d scenes. *IEEE Transactions on Pattern Analysis and Machine Intelligence*, 21(5):433–449, 1999.
- [10] Alex Kendall and Yarin Gal. What uncertainties do we need in bayesian deep learning for computer vision? In *Proceedings of the 31st International Conference on Neural Information Processing Systems, NIPS’17*, page 5580–5590, 2017. ISBN 9781510860964.
- [11] Bernhard Kerbl, Georgios Kopanas, Thomas Leimkühler, and George Drettakis. 3d gaussian splatting for real-time radiance field rendering. *ACM Transactions on Graphics*, 42(4), 2023. Proc. SIGGRAPH.
- [12] Soonbin Lee, Yeong-Gyu Kim, Simon Sasse, Tomas M. Borges, Yago Sanchez, Eun-Seok Ryu, Thomas Schierl, and Cornelius Hellge. Gaussianpop: Principled simplification framework for compact 3d gaussian splatting via error quantification. *arXiv preprint arXiv:2602.06830*, 2026. doi: arXiv.2602.06830.
- [13] Yangzhi Ma, Bojun Liu, Jie Li, Li Li, and Dong Liu. Hash grid feature pruning. *arXiv preprint arXiv:2512.22882*, 2025. doi: 10.48550/arXiv.2512.22882.
- [14] Ben Mildenhall, Pratul P. Srinivasan, Matthew Tancik, Jonathan T. Barron, Ravi Ramamoorthi, and Ren Ng. Nerf: representing scenes as neural radiance fields for view synthesis. *Commun. ACM*, 65(1):99–106, December 2021. ISSN 0001-0782. doi: 10.1145/3503250. URL <https://doi.org/10.1145/3503250>.
- [15] Subhankar Mishra. Clean-gs: Semantic mask-guided pruning for 3d gaussian splatting. *arXiv preprint arXiv:2601.00913*, 2026.
- [16] Stéphane Pateux, Matthieu Gendrin, Luce Morin, Théo Ladune, and Xiaoran Jiang. Bogauss: Better optimized gaussian splatting. *arXiv preprint arXiv:2504.01844*, 2025. doi: 10.48550/arXiv.2504.01844.

- [17] Charles R. Qi, Li Yi, Hao Su, and Leonidas J. Guibas. Pointnet++: deep hierarchical feature learning on point sets in a metric space. In *Proceedings of the 31st International Conference on Neural Information Processing Systems*, NIPS'17, page 5105–5114, 2017. ISBN 9781510860964.
- [18] Shiyu Qiu, Chunlei Wu, Zhenghao Wan, and Siyuan Tong. High-fold 3d gaussian splatting model pruning method assisted by opacity. *Applied Sciences*, 15(3):1535, 2025. doi: 10.3390/app15031535.
- [19] AmirHossein Naghi Razlighi, Elaheh Badali Golezani, and Shohreh Kasaei. Confident splatting: Confidence-based compression of 3d gaussian splatting via learnable beta distributions. *arXiv preprint arXiv:2506.22973*, 2025. doi: arXiv.2506.22973.
- [20] Radu Bogdan Rusu, Nico Blodow, and Michael Beetz. Fast point feature histograms (fpfh) for 3d registration. In *ICRA*, pages 3212–3217, 2009.
- [21] Hui Shuai, Yucheng Shi, Yubao Sun, and Qingshan Liu. Adversarial pruning networks for compact 3d gaussian splatting. *IEEE Transactions on Multimedia*, pages 1–10, 2025. doi: 10.1109/TMM.2025.3632681.
- [22] Federico Tombari, Samuele Salti, and Luigi Di Stefano. Unique signatures of histograms for local surface description. In *ECCV*, pages 356–369, 2010.
- [23] Xiufeng Xie, Riccardo Gherardi, Zhihong Pan, and Stephen Huang. Hollownerf: Pruning hashgrid-based nerfs with trainable collision mitigation. In *ICCV*, 2023.
- [24] Yuwen Xiong, Mengye Ren, and Raquel Urtasun. Loco: local contrastive representation learning. In *Proceedings of the 34th International Conference on Neural Information Processing Systems*, NIPS '20, 2020. ISBN 9781713829546.
- [25] Kaifa Yang, Qi Yang, Yiling Xu, and Zhu Li. Rap: Fast feedforward rendering-free attribute-guided primitive importance score prediction for efficient 3d gaussian splatting processing. *arXiv preprint arXiv:2602.19753*, 2026. doi: <https://arxiv.org/abs/2602.19753>.
- [26] Zhaoliang Zhang, Tianchen Song, Yongjae Lee, Li Yang, Cheng Peng, Rama Chellappa, and Deliang Fan. Lp-3dgs: Learning to prune 3d gaussian splatting. In *NeurIPS*, 2024.